

Atomic Resolution Crystal Field Splitting Mapping in Polar Vortices Oxide Superlattices

Sandhya Susarla¹, Sujit Das², Weichuan Huang², Colin Ophus¹, Peter Ercius¹ and Ramamoorthy Ramesh²

¹Lawrence Berkeley National Laboratory, Berkeley, California, United States, ²University of California-Berkeley, Berkeley, California, United States

Novel topological phases such as polar vortices and skyrmions in the complex oxide systems have generated enormous interest in the condensed matter physics community due to their exotic properties like negative capacitance and chiral domains.^{1–4} One such topological form; polar vortices have been recently identified in PbTiO₃/SrTiO₃ (PTO/STO) superlattices grown on DyScO₃ (DSO) by controlling of elastic, electrostatic and gradient energy.² The atomic structure of polar vortices have been studied using four-dimensional scanning transmission electron microscopy (4D-STEM) and reciprocal space mapping (RSM) but these techniques do not probe electronic structure changes like crystal field splitting and spin-orbit coupling.^{2,5} To some extent, the chiral nature of the polar vortices has been probed using X-Ray circular dichroism (XCD) but the lack of spatial resolution still limits the measurement to a certain extent.³ Electron energy near edge spectroscopy (ELNES) allows us to probe the K, L and M edges of transition metals; giving information about the spin-orbit coupling and crystal field splitting. With the continuously changing polarization in vortices, ELNES provides an ideal platform to study local electronic structure changes. Measuring spin-orbit coupling and crystal field splitting requires STEM-EELS mapping at atomic resolution with extremely high signal to noise.

We have studied the crystal field splitting of Titanium (Ti) L-edge in the PTO/STO vortices grown by pulsed laser deposition. High resolution STEM-EELS mapping was performed using TEAM I at Lawrence Berkeley National Laboratory. Monochromated (~0.2 eV FWHM) electron energy loss spectroscopy (mono-EELS) measurements were performed using a Gatan K3 camera installed in a Gatan Continuum GIF. Spectra were de-noised using principle component analysis (PCA) where the first 3 components were used.⁶

Figure 1a shows the HAADF-STEM image of 15x15 unit cells of PTO/STO superlattice. Vortices in the superlattices were identified by A-Site Pb column position fitting. The B sites were not intense enough to accurately determine the displacement. However, these polar vortices also have slight A site displacement as consequence of the B site displacement. Figure 1b shows the relative displacement of Pb atoms with respect to conventional PbTiO₃. The red color indicates leftward displacement whereas the blue color indicated the rightward displacement. The core of the vortices is present at the border of red and blue regions. We can also notice the vortices region as slight dark contrast in PTO layer in the HR-HAADF-STEM image shown in Figure 1a (indicated by white dashes). The vortex regions were mapped by STEM-EELS to determine the local changes in the Ti L edge. Figure 1c shows the simultaneously acquired HAADF-STEM image acquired during the EELS mapping. Figure 1d shows the PCA enhanced EELS spectra taken from the vortex, PTO and STO respectively. Ti L edge measures the delocalization of electrons in 2p_{2/3} and 2p_{1/3} to 3d levels as L₃ and L₂ transitions. In case of the O_h symmetry there is crystal field splitting as t_{2g} and e_g due to strong spin-orbit coupling of the transition metal. Crystal field

splitting in the Ti L edge decreases from STO to PTO as the symmetry changes from O_h to D_{4h} . However, as we enter the vortex region, the e_g peak of the L_3 Ti edge further splits into two peaks. The e_g peak in the L_3 Ti L edge indicates the hybridization of d_{z^2} and $d_{x^2-y^2}$ orbitals of Ti with O 2p. Usually the e_g peak is split in cases of unstrained PTO. A previous theoretical report indicates that this splitting is caused by the paraelectric nature of tetragonal PTO.⁷

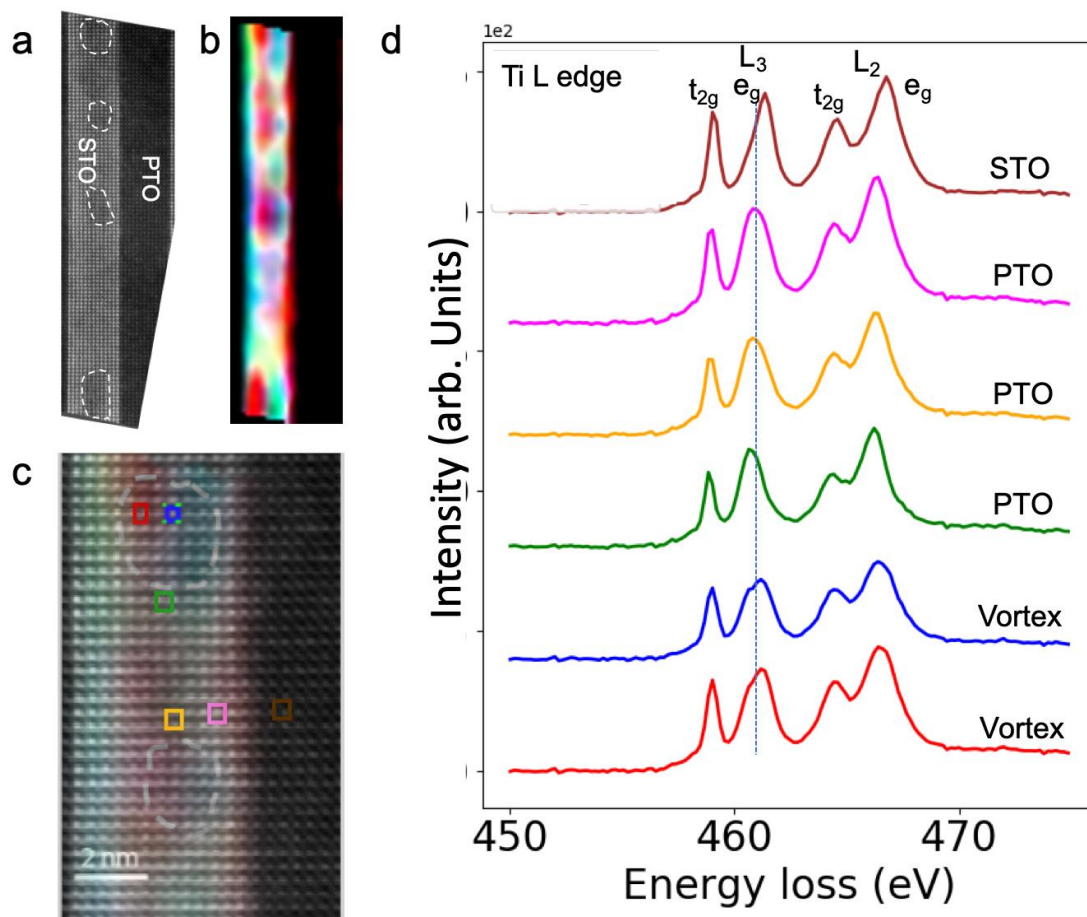


Figure 1. a) Atomic resolution drift corrected HAADF-STEM image of PTO/STO superlattice. b) A-site fitting maps showing the relative displacement of A sites in the vortices. The red color represents left shift and the blue color represents right shift. The vortices are located in between the red and blue regions. c) Simultaneously acquired HAADF-STEM image during EELS scans. The displacement maps in (b) are superimposed on the image. d) Series of EELS spectra extracted from boxes indicated in (c). Inside the vortices region, the e_g peak of the Ti L edge splits into 2 peaks.

References

1. Das, S. *et al.* Observation of room-temperature polar skyrmions. *Nature* **568**, 368–372 (2019).
2. Yadav, A. K. *et al.* Observation of polar vortices in oxide superlattices. *Nature* **530**, 198–201 (2016).
3. Shafer, P. *et al.* Emergent chirality in the electric polarization texture of titanate superlattices. *Proc. Natl. Acad. Sci.* **115**, 915–920 (2018).
4. Yadav, A. K. *et al.* Spatially resolved steady-state negative capacitance. *Nature* **565**, 468–471 (2019).
5. Li, Q. *et al.* Quantification of flexoelectricity in $PbTiO_3/SrTiO_3$ superlattice polar vortices using machine learning and phase-field modeling. *Nat. Commun.* **8**, 1–8 (2017).

6. Muller, D. A. *et al.* Atomic-Scale Chemical Imaging of Composition and Bonding by Aberration-Corrected Microscopy. *Science*, **319**, 1073 LP – 1076 (2008).
7. Torres-Pardo, A. *et al.* Spectroscopic mapping of local structural distortions in ferroelectric PbTiO₃/SrTiO₃ superlattices at the unit-cell scale. *Phys. Rev. B* **84**, 220102 (2011).